arXiv:1212.3554v1 [hep-ph] 14 Dec 2012

DESY 12-199

Baryogenesis, Dark Matter and the Maximal Temperature of the Early Universe*

Wilfried Buchmüller

Deutsches Elektronen-Synchrotron DESY, Hamburg, Germany

Mechanisms for the generation of the matter-antimatter asymmetry and dark matter strongly depend on the reheating temperature T_R, the maximal temperature reached in the early universe. Forthcoming results from the LHC, low energy experiments, astrophysical observations and the Planck satellite will significantly constrain baryogenesis and the nature of dark matter, and thereby provide valuable information about the very early hot universe. At present, a wide range of reheating temperatures is still consistent with observations. We illustrate possible origins of matter and dark matter with four examples: moduli decay, electroweak baryogenesis, leptogenesis in the νMSM and thermal leptogenesis. Finally, we discuss the connection between baryogenesis, dark matter and inflation in the context of supersymmetric spontaneous B-L breaking.

PACS numbers: 11.30.Fs, 05.30.-d, 95.30.Cq, 98.80.Cq

1. Introduction

Let us begin by recalling some temperatures, possibly realized in the hot early universe, the related cosmic times, and the connection with microscopic physics at the corresponding energies:

- $T_R \sim 0.1$ eV $[t \sim 10^{13}$ s]
  Light nuclei and electrons form neutral atoms and the universe becomes transparent to photons. They decouple from the plasma and are observable today as cosmic microwave background (CMB).

* Lectures presented at the LII Cracow School of Theoretical Physics, *Astroparticle Physics in the LHC Era*, May 19-27, 2012, Zakopane, Poland

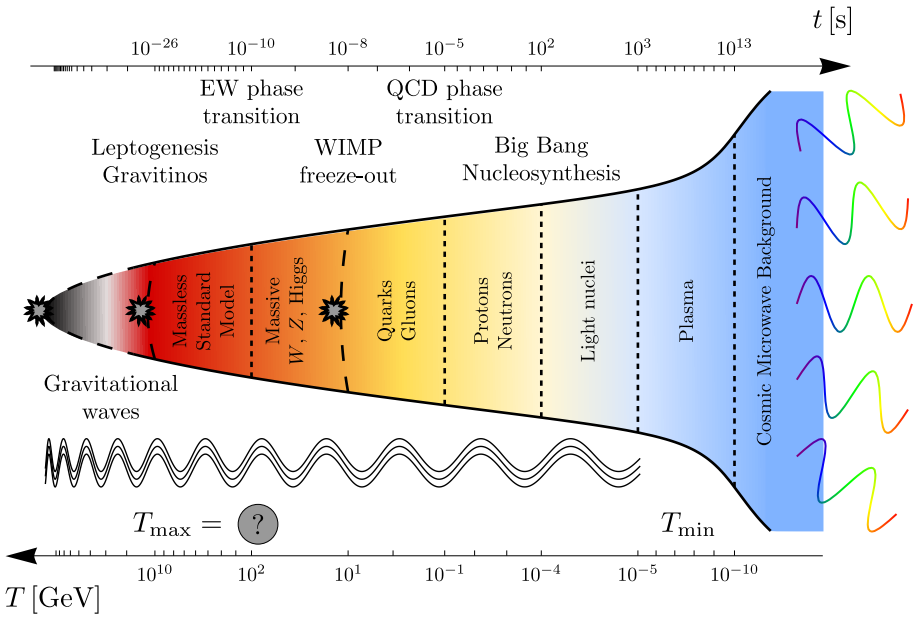

Fig. 1. Epochs of the hot early universe, their cosmic time scales (top) and temperatures (bottom). From Ref. [4].

- $T_R \simeq 0.1 \ldots 10$ MeV[1] $[t \simeq 10^2 \ldots 10^{-2}$ s]
  Light nuclei are formed from protons and neutrons (primordial nucleosynthesis, BBN) and neutrinos decouple from the plasma.

- $T_R \sim 10$ GeV $[t \sim 10^{-8}$ s]
  Weakly interacting massive particles (WIMPs), the most popular dark matter candidates, decouple from the plasma.

- $T_R \sim 100$ GeV $[t \sim 10^{-10}$ s]
  The Higgs vacuum expectation value forms, and all Standard Model particles become massive. Baryon and lepton number changing 'sphaleron processes' are no longer in thermal equilibrium.

- $T_R \sim 10^8 \ldots 10^{11}$ GeV $[t \sim 10^{-22} \ldots 10^{-28}$ s]
  Baryogenesis via leptogenesis takes place and gravitino dark matter can be thermally produced.

- $T_R \sim 10^{12}$ GeV $[t \sim 10^{-30}$ s] In supersymmetric theories with extra dimensions one expects that the present 'vacuum' of the universe is metastable [2]. To avoid a rapid transition to a supersymmetric flat

[1] In natural units $\hbar = c = k_B = 1$ one has 1 eV = 1.16 10^4K.

higher-dimensional ground state, the reheating temperature cannot exceed a 'maximal' reheating temperature $T_R^{\max}$. For gravitino masses $m_{3/2} = \mathcal{O}(\text{TeV})$, one estimates in string theories $T_R^{\max} \sim 10^{12}$ GeV [3].

The epochs of the hot early universe described above are illustrated in Fig. 1. The CMB provides us with detailed information about the final stage of the hot phase. Hence, the reheating temperature must have exceeded ~ 0.1 eV. Furthermore, the success of primordial nucleosynthesis suggests that the reheating temperature has reached ~ 10 MeV. Here our present knowledge ends. Progress will crucially depend on how much the various possibilities for baryogenesis and dark matter candidates can be narrowed down. The following four examples illustrate the impact on the reheating temperature T_R. It would be most fascinating to obtain direct information about the beginning of the hot early universe, which may eventually be achieved by means of gravitational waves [5].

2. Example I: Moduli Decay

Let us first consider an example [6] with a very low reheating temperature, $T_R \sim 100$ MeV, just above the temperature required by BBN. The theoretical framework is a supersymmetric extension of the Standard Model with a heavy 'modulus field', which is typical for string compactifications. The initial energy density of the universe is dominated by coherent oscillations of the modulus field, with an equation of state corresponding to nonrelativistic matter.

The modulus superfield $\Phi = (\phi, \widetilde{\phi}, F_\phi)$ is assumed to couple to matter fields via a specific nonrenormalizable interaction in the superpotential, suppressed by an inverse power of the Planck mass $M_{\rm P}$,

$$W \supset \frac{1}{M_{\rm P}} \Phi(UDD) \; , \tag{2.1}$$

where $U = (\widetilde{u}^c, u^c, F_u)$ and $D = (\widetilde{d}^c, d^c, F_d)$ denote up- and down-type quark superfields, respectively. The ϕ charge density, the difference between the number densities ϕ and anti-ϕ particles, is given by

$$q_\phi = n_\phi - n_{\phi^*} = i \left(\dot{\phi}^* \phi - \phi^* \dot{\phi} \right) \; . \tag{2.2}$$

The time evolution of modulus field and charge density are determined by the equations of motion (H: Hubble rate, Γ_ϕ: decay rate),

$$\ddot{\phi} + (3H + \Gamma_\phi)\, \dot{\phi} + \frac{\partial V}{\partial \phi^*} \; = \; 0 \; , \tag{2.3}$$

$$\dot{q}_\phi + 3H\, q_\phi \; = \; -i \left(\phi \frac{\partial V}{\partial \phi} - \phi^* \frac{\partial V}{\partial \phi^*} \right) \; , \tag{2.4}$$

where H and Γ_ϕ denote Hubble parameter and ϕ-decay rate, respectively. The scalar potential contains a ϕ mass term, some polynomial $F(|\phi|^2/{M_\mathrm{P}}^2)$ and a power of ϕ that is determined by a discrete symmetry,

$$V = m_\phi^2|\phi|^2 + {m_{3/2}}^2 M_\mathrm{p}^2 F(|\phi|^2/M_\mathrm{p}^2) + \left(\kappa\,\frac{m_{3/2}^2}{M_\mathrm{p}^4}\,\phi^6 + \mathrm{h.c.}\right) + \ldots, \quad (2.5)$$

where $\kappa = \mathcal{O}(1)$ and $m_{3/2}$ is the gravitino mass.

During inflation the modulus field develops an expectation value $\phi_\mathrm{ini} \sim M_\mathrm{p}$ with a phase $\mathcal{O}(1)$. This condensate stores a charge density. Integrating the field equations from the initial state with $H \gg m_\phi$ up to $t_\phi = m_\phi^{-1}$, one obtains for the charge density

$$q_\phi(t_\phi) \;\sim\; |\kappa|\,\frac{m_{3/2}^2}{2m_\phi\,M_\mathrm{p}^4}\,\phi_\mathrm{ini}^6\;. \quad (2.6)$$

The number density of ϕ particles is determined by the energy density of the ϕ field,

$$n_\phi + n_{\phi^*} \simeq \frac{\rho_\phi}{m_\phi} = \frac{1}{m_\phi}\left(m_\phi^2\,|\phi|^2 + |\dot\phi|^2\right)\;, \quad (2.7)$$

from which one obtains for the ϕ charge asymmetry:

$$\varepsilon = \frac{n_\phi - n_{\phi^*}}{n_\phi + n_{\phi^*}} = \frac{q_\phi}{n_\phi + n_{\phi^*}} \sim |\kappa|\,\left(\frac{m_{3/2}}{m_\phi}\right)^2\;. \quad (2.8)$$

For $\phi < M_\mathrm{P}$, baryon number is approximately conserved, and the ϕ asymmetry becomes a baryon asymmetry in ϕ decays such as $\phi^* \to u\widetilde{dd}$.

The ϕ decay width is given by

$$\Gamma_\phi \;=\; \xi\,\frac{m_\phi^3}{M^2}\;, \quad \xi = 10^{-3}\ldots 10^{-2}\;, \quad (2.9)$$

for a coefficient $\mathcal{O}(1)$ in Eq. (2.1). Assuming 'instant reheating', one obtains from the definition $H(T_R) = \Gamma_\phi$ the reheating temperature

$$\begin{aligned} T_R \;&\simeq\; \left(\frac{90}{\pi^2 g_*}\right)^{1/2}\sqrt{\Gamma M_\mathrm{P}} \\ &\simeq\; 120\ \mathrm{MeV}\left(\frac{\xi}{10^{-2}}\right)^{1/2}\left(\frac{m_\phi}{1500\,\mathrm{TeV}}\right)^{3/2}\;, \end{aligned} \quad (2.10)$$

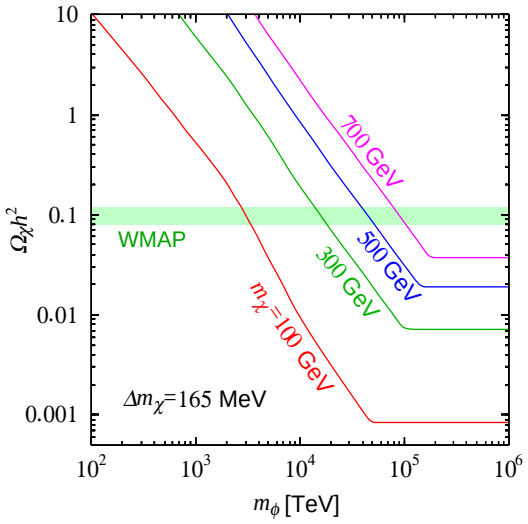

Fig. 2. $\Omega_\chi h^2$ as function of the modulus mass m_ϕ for various wino masses m_χ. From Ref. [6]

where we have used $\sqrt{\pi^2 g_*/90} \simeq 1$ for temperatures of order MeV. Until they decay, ϕ particles dominate the energy density of the universe, which relates their number density just before the decay to the reheating temperature,

$$m_\phi (n_\phi + n_{\phi^*}) \simeq \frac{\pi^2}{30} g_* T_R^4 \,. \tag{2.11}$$

Using Eq. (2.10), one then obtains the baryon asymmetry in terms of ϕ asymmetry, ϕ mass and reheating temperature,

$$\begin{aligned} \frac{n_b}{s} &\simeq \frac{3}{4}\,\varepsilon\,\frac{T_d}{m_\phi} \\ &\sim 10^{-10}\,|\kappa| \left(\frac{\xi}{10^{-2}}\right)^{1/2} \left(\frac{m_{3/2}}{50\ \mathrm{TeV}}\right)^2 \left(\frac{m_\phi}{1500\,\mathrm{TeV}}\right)^{-3/2} . \end{aligned} \tag{2.12}$$

Clearly, for a very heavy gravitino, as predicted by anomaly mediation [7,8], and an even heavier modulus field ϕ, the observed baryon asymmetry can be generated in ϕ decays.

The lightest supersymmetric particle (LSP) is a natural dark matter candidate. It can be a higgsino or wino, as predicted in anomaly mediation. Approximately one LSP is produced per ϕ decay. The LSP density is reduced by pair annihilation, and solving a set of Boltzmann equations leads

to the prediction for the dark matter abundance [6].

$$\Omega_\chi h^2 \simeq 0.1 \left(\frac{3\times 10^{-3}}{m_\chi^2\langle\sigma v\rangle}\right)\left(\frac{10^{-2}}{\xi}\right)^{1/2}\left(\frac{m_\chi}{100\mathrm{GeV}}\right)^3\left(\frac{m_\phi}{1500\mathrm{TeV}}\right)^{-3/2}. \quad (2.13)$$

In anomaly mediation, one has for the wino LSP, $m_\chi/m_{3/2} \sim g_2^2/(16\pi^2)$. In the ratio of dark matter abundance and baryon asymmetry the dependence on the ϕ mass drops out, and one obtains

$$\frac{\Omega_\chi}{\Omega_b} \;\sim\; |\kappa|^{-1}\times 10^{-2}\times\frac{m_\chi}{m_{\mathrm{nucleon}}}\;. \quad (2.14)$$

For $m_\chi = \mathcal{O}(100\ \mathrm{GeV})$ the observed ratio $\Omega_{\mathrm{CDM}}/\Omega_b \simeq 5$ is easily accomodated. The observed dark matter abundance imposes a constraint on LSP and modulus masses, which is illustrated in Fig. 2.

The example of modulus decay nicely illustrates that a reheating temperature as small as $T_R \sim 100$ MeV is sufficient for a consistent picture of primordial nucleosynthesis, baryogenesis and dark matter. On the other hand, the predictive power of the model is rather limited. Two observables, Ω_b and Ω_{DM} are related to four new parameters, $m_{3/2}$, m_ϕ, κ and ξ. In addition, the initial value ϕ_{ini} of the modulus field has to be postulated. The model then yields the composition of the primordial plasma at a temperature $T_R \sim 100$ MeV. It would be very interesting to identify further comological predictions of the model.

3. Example II: Electroweak Baryogenesis

3.1. The High-Temperature Phase of the Standard Model

Most mechanisms of baryogenesis make use of some noneqilibrium process in the hot early universe, such as the decay of heavy particles or cosmological phase transitions. One then has to satisfy Sakharov's conditions for particle interations and cosmological evolution [9],

- baryon number violation,
- C and CP violation,
- deviation from thermal equilibrium.

Even if these conditions are fulfilled, further severe quantitative constraints must usually be satisfied to obtain the observed matter-antimatter asymmetry. This is well illustrated by the example presented in Sakharov's original paper: Superheavy 'maximons' with mass $\mathcal{O}(M_{\mathrm{P}})$ decay at an initial temperature $T_i \sim M_{\mathrm{P}}$ with a CP violation related to the CP violation in

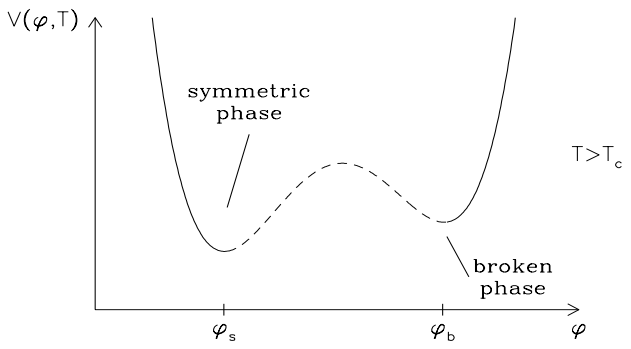

Fig. 3. The finite-temperature effective potential of the Higgs field above the critical temperature, i.e. $T > T_c$. ϕ_s and ϕ_b correspond to symmetric and Higgs (broken) phase.

K^0-decays, and the violation of baryon number leads to a proton lifetime $\tau_p > 10^{50}$ years, much larger than current estimates in grand unified theories.

The theory of baryogenesis crucially depends on nonperturbative properties of the standard model, first of all the nature of the electroweak transition. Depending on the temperature, the symmetric phase or the broken phase represents the global minimum (cf. Fig. 3). At the critical temperature T_c both phases are degenerate. At temperatures just above (below) T_c, a first-order phase transition can occur from the symmetric (broken) to the broken (symmetric) phase. A measure for the strength of the transition is the jump in the expectation value of the Higgs field,

$$v_T = \sqrt{\phi_b^\dagger \phi_b}\Big|_T - \sqrt{\phi_s^\dagger \phi_s}\Big|_T \,. \tag{3.1}$$

A comparison between perturbative and lattice calculations of v_T at $T = T_c$ is shown in Fig. 4a. There is remarkable agreement between lattice simulations for the full four-dimensional theory at finite temperature, for the effective three-dimensional theory corresponding to the high-temperature limit, and resummed perturbation theory.

The perturbative result for v_T shows a smooth decrease for Higgs masses up to 80 GeV. This behaviour, however, is not correct since for large Higgs masses nonperturbative effects become important, which turn the first-order phase transition into a smooth crossover for Higgs masses larger than $m_H^c = \mathcal{O}(m_W)$. This behaviour has first been demonstrated by solving

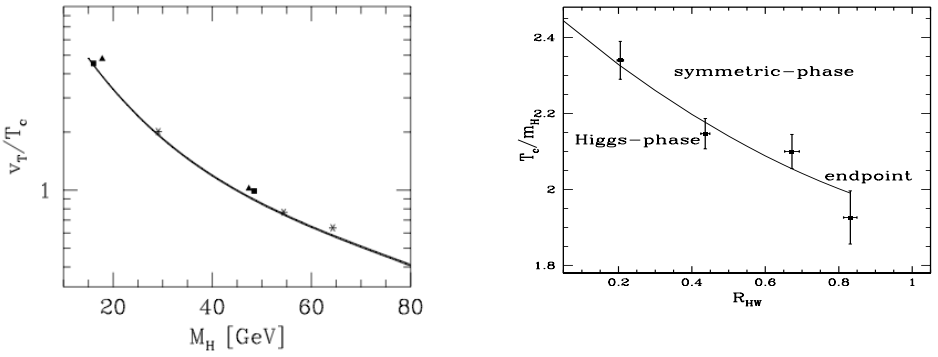

Fig. 4. (a) (left) Jump of the Higgs expectation value at the critical temperature as function of the Higgs mass. Comparison of four-dimensional lattice simulations (triangles, squares) [11] with three-dimensional lattice simulations (stars) [12] and resummed perturbation theory [13]. From Ref. [14]. (b)(right) Critical temperature as function of Higgs/W-boson mass ratio $R_{HW} = m_H/m_W$ from four-dimensional lattice simulations. From Ref. [17].

gap equations for the Higgs model [15] and then by three-dimensional lattice simulations [16]. The result of four-dimensional lattice simulations [17] is displayed in Fig. 4b, which gives T_c/m_H as function of the Higgs mass in units of the W-boson mass, $R_{HW} = m_H/m_W$. The line of first-order phase transitions for small Higgs masses has an endpoint corresponding to a second order phase transition. The corresponding critical Higgs mass is $m_H^c = 72.1 \pm 1.4$ GeV [18]. For larger Higgs masses the electroweak transition is a smooth crossover. Critical temperature and critical Higgs mass can be estimated by requiring that the perturbative vector boson mass $m = gv_T$ is equal to the nonperturbative finite-temperature magnetic mass, obtained by solving gap equations, $m_{SM} = Cg^2T$, with $C \simeq 0.35$ [19,20]. This yields for the critical Higgs mass [21]

$$m_H^c = \left(\frac{3}{4\pi C}\right)^{1/2} m_W \simeq 74 \text{ GeV} . \tag{3.2}$$

The critical Higgs mass is far below the mass of 126 GeV of the Higgs-like boson recently discovered at the LHC [22]. If this boson is indeed the Higgs particle of the Standard Model, then we know that there has been no departure from themal equilibrium during the cosmological electroweak

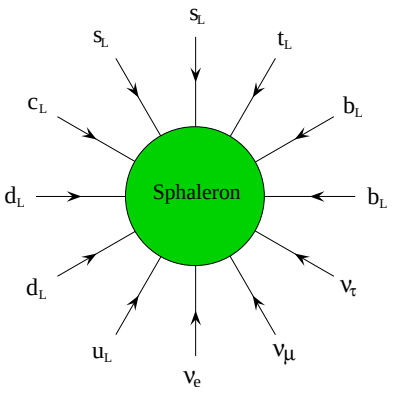

Fig. 5. One of the 12-fermion processes which are in thermal equilibrium in the high-temperature phase of the standard model.

transition.

The second crucial nonperturbative aspect of baryogenesis is the connection between baryon number and lepton number in the high-temperature, symmetric phase of the Standard Model. Due to the chiral nature of the weak interactions B and L are not conserved [23]. At zero temperature this has no observable effect due to the smallness of the weak coupling. However, as the temperature reaches the critical temperature T_c of the electroweak phase transition, B and L violating processes come into thermal equilibrium [24]. The rate of these processes is related to the free energy of sphaleron-type field configurations which carry topological charge. In the standard model they lead to an effective interaction of all left-handed fermions [23] (cf. Fig. 5),

$$O_{B+L} = \prod_i (q_{Li} q_{Li} q_{Li} l_{Li}) \ , \tag{3.3}$$

which violates baryon and lepton number by three units,

$$\Delta B = \Delta L = 3 \ . \tag{3.4}$$

The sphaleron transition rate in the symmetric high-temperature phase has been evaluated by combining an analytical resummation with numerical lattice techniques [25]. The result is, in accord with previous estimates, that B and L violating processes are in thermal equilibrium for temperatures in the range

$$T_{EW} \sim 100 \text{ GeV} < T < T_{SPH} \sim 10^{12} \text{ GeV} \ . \tag{3.5}$$

Although uncontroversial among theorists, it has to be stressed that this important phenomenon has so far not been experimentally tested! It is therefore very interesting that the corresponding phenomenon of chirality changing processes in strong interactions might be observable in heavy ion collisions at the LHC [26, 27].

Sphaleron processes relate baryon and lepton number and therefore strongly affect the generation of the cosmological baryon asymmetry. Analyzing the chemical potentials of quarks and leptons in thermal equilibrium [28], one obtains an important relation between the asymmetries in B-, L- and B-L-number,

$$\langle B\rangle_T = c_S\langle B-L\rangle_T = \frac{c_S}{c_S-1}\langle L\rangle_T \ , \tag{3.6}$$

where $c_S = \mathcal{O}(1)$. In the Standard Model one has $c_s = 28/79$.

This relation suggests that lepton number violation can explain the cosmological baryon asymmetry. However, lepton number violation can only be weak at late times, since otherwise any baryon asymmetry would be washed out. The interplay of these conflicting conditions leads to important contraints on neutrino properties, and on extensions of the Standard Model in general. Because of the sphaleron processes, lepton number violation can replace baryon number violation in Sakharov's conditions for baryogenesis.

3.2. Composite Higgs Model

Baryogenesis requires departure from thermal equilibrium. As discussed in the previous section, due to the large Higgs mass the electroweak transition in the Standard Model does not provide the necessary noneqilibrium for electroweak baryogenesis. However, in extensions of the Standard Model with a strongly interacting Higgs sector, sufficiently strong first-order electroweak phase transitions [29] and electroweak baryogenesis are possible [30].

As an example, consider a strongly interacting theory where a global $SO(6)$ symmetry is spontaneously broken to the subgroup $SO(5)$, such that the Higgs doublet together with an additional singlet s arise as pseudo-Goldstone bosons. In unitary gauge, the finite-temperature potential for the Higgs field h and the singlet s can be written as [30],

$$V(h,s,T) \ = \ \frac{\lambda_h}{4}\left[h^2 - v_c^2 + \frac{v_c^2}{w_c^2}s^2\right]^2 + \frac{\kappa}{4}\,s^2h^2 \tag{3.7}$$

$$+\frac{1}{2}(T^2-T_c^2)(c_h\,h^2 + c_s\,s^2) \ , \tag{3.8}$$

where v_c, w_c, κ, c_h and c_s are parameters of the model. For realistic

	m_h	m_s	v_c	f/b	$L_w v_c$	v_c/T_c
S1	120 GeV	81 GeV	188 GeV	1.88 TeV	7.1	2.0
S2	140 GeV	139.2 GeV	177.8 GeV	1.185 TeV	3.5	1.5

Table 1. Two numerical examples of models with viable eletroweak baryogenesis; m_h and m_s are the Higgs and singlet masses, respectively. From Ref. [30].

Higgs masses, a sufficiently strong first-order phase transition is achieved, satisfying the necessary condition for the jump in the Higgs field $v_c/T_c > 1$ (cf. Table 1).

The cosmological first-order phase transition proceeds via nucleation and growth of bubbles [31]. This provides the necessary departure from thermal equilibrium. *CP*-violating reflections and transmissions at the bubble surface then generate an asymmetry in baryon number (cf. Fig. 6) , and for a sufficiently strong phase transition this asymmetry is frozen in the true vacuum inside the bubble

In the considered model, *CP*-violating couplings of top-quarks to the two Higgs bosons H and s are responsible for the generation of a baryon asymmetry,

$$\mathcal{L}_{tHS} = \frac{s}{f} H \bar{Q}_3 (a + ib\gamma_5) t + \text{h.c.} \; . \tag{3.9}$$

Detailed calculations show that the observed baryon asymmetry can be explained for a sufficiently strong coupling.

The *CP*-violating top-quark couplings induce via higher-order loops electric dipole moments for neutron and electron (cf. Fig. 7) , which are severely constrained, $d_e/e < 1.05 \times 10^{-27}$cm and $d_n/e < 2.9 \times 10^{-26}$cm [32]. Furthermore,

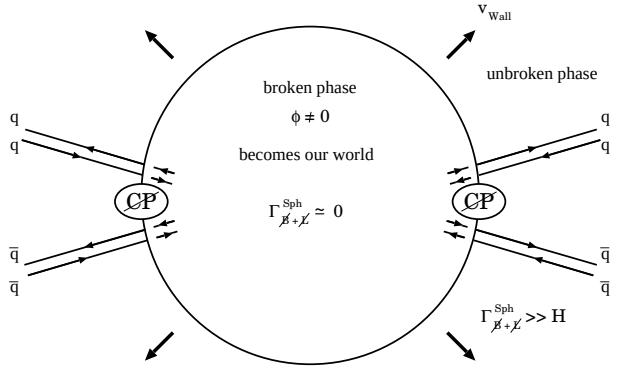

Fig. 6. Sketch of nonlocal electroweak baryogenesis. From Ref. [31].

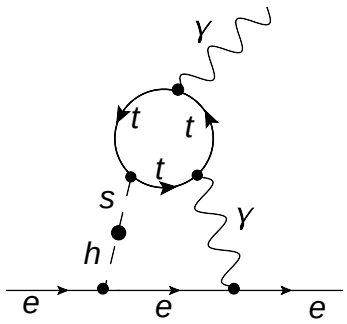

Fig. 7. Dominant two-loop contribution to electron electric dipole moment, induced by *CP* violating top-quark couplings. From Ref. [30].

stringent constraints from electroweak precision observables have to be satisfied. A consistent picture can be obtained for Higgs masses in the range from 100 GeV to 150 GeV, in agreement with the evidence for a Higgs-like particle at the LHC. Note that the considered model in its simplest form does not have a dark matter candidate. This can be changed by extending the model to include another, 'inert' Higgs doublet. The required reheating temperature for baryogenesis is the electroweak scale, $T_R \sim T_{EW} \sim 100$ GeV.

Electroweak baryogenesis in the minimal supersymmetric standard model (MSSM) has been a very popular scenario after it became clear that baryogenesis was impossible in the non-supersymmetric Standard Model. It turns out, however, that due to recent results from the LHC rather extreme stop masses are required to make baryogenesis possible, $m_{\tilde{t}_R} \lesssim 110$ GeV with $m_{\tilde{t}_L} \gtrsim 50$ TeV [33], and it appears likely that electroweak baryogenesis will soon be ruled out also in the MSSM.

4. Example III: Baryogenesis in the νMSM

At temperatures around the electroweak scale, sphaleron processes come into thermal equilibrium and baryon number violation can therefore be replaced by lepton number violation. This occurs in the Standard Model supplemented by Majorana (sterile) neutrinos. Baryogenesis can then take place via leptogenesis [34]. It is remarkable that for small neutrino masses of order GeV or keV, such a model (νMSM scenario) can account not only for neutrino oscillations, but also for baryogenesis and dark matter [35].

The starting point is the familar Standard Model Lagrangian extended

by Dirac and Majorana mass terms,

$$\begin{aligned}\mathcal{L}_{\nu MSM} &= \mathcal{L}_{SM} - \bar{L}_L F \nu_R \tilde{\Phi} - \bar{\nu}_R F^\dagger L_L \tilde{\Phi}^\dagger \\ &\quad -\frac{1}{2}(\bar{\nu_R^c} M_M \nu_R + \bar{\nu}_R M_M^\dagger \nu_R^c) \ . \end{aligned} \tag{4.1}$$

Here M_M is the Majorana mass matrix of the right-handed neutrinos ν_R, and the Higgs expectation value $\langle\Phi\rangle = v$ generates the Dirac neutrino mass matrix $m_D = Fv$. The light and heavy neutrino mass eigenstates ν_i and N_I have masses m_i and M_I, respectively. A crucial quantity for phenomenology is the active-sterile mixing matrix $\theta = m_D M_M^{-1}$, with $U^2 = \mathrm{tr}(\theta^\dagger\theta)$.

Recently, the scenario has been studied in detail quantitatively [36]. The lightest sterile neutrino N_1 provides dark matter, with a mass in the range 1 keV $< M_1 \lesssim$ 50 keV, and tiny mixings, $10^{-13} \lesssim \sin^2(2\theta_{\alpha 1}) \lesssim 10^{-7}$, constrained by X-ray observations. The allowed and excluded parameter regions are shown in Fig. 8. Along the solid lines the model reproduces the observed value of $\Omega_{\rm DM}$ for the indicated chemical potentials.

Following Ref. [37], baryogenesis is achieved by *CP*-violating oscillations of N_2 and N_3, which are thermally produced at temperature $T \gtrsim T_{EW} \sim$ 140 GeV (assuming a Higgs mass $m_H = 126$ GeV). The time evolution of the $N_{2,3}$ density matrices ρ_N and $\rho_{\bar{N}}$ and the lepton chemical potentials μ_α are described by the kinetic equations [36]

$$i\frac{d\rho_N}{dT} = [H, \rho_N] - \frac{i}{2}\{\Gamma_N, \rho_N - \rho^{eq}\} + \frac{i}{2}\mu_\alpha \tilde{\Gamma}_N^\alpha \ , \tag{4.2}$$

$$i\frac{d\rho_{\bar{N}}}{dT} = [H^*, \rho_{\bar{N}}] - \frac{i}{2}\{\Gamma_N^*, \rho_{\bar{N}} - \rho^{eq}\} - \frac{i}{2}\mu_\alpha \tilde{\Gamma}_N^{\alpha *} \ , \tag{4.3}$$

$$\begin{aligned} i\frac{d\mu_\alpha}{dT} &= -i\Gamma_L^\alpha \mu_\alpha + i\mathrm{tr}\left[\tilde{\Gamma}_L^\alpha(\rho_N - \rho^{eq})\right] \\ &\quad -i\mathrm{tr}\left[\tilde{\Gamma}_L^{\alpha *}(\rho_{\bar{N}} - \rho^{eq})\right] \ . \end{aligned} \tag{4.4}$$

Here ρ^{eq} is the equilibrium density matrix, H is the dispersive part of the finite temperature effective Hamiltonian for the N_I and Γ_N, Γ_L^α and $\tilde{\Gamma}_L^\alpha$ are rates accounting for different dissipative effects. The equations describe thermal sterile neutrino production, oscillations, freeze-out and decay.

To obtain the right amount of baryon asymmetry, resonant enhancement of *CP* violation is needed, with a very high mass degeneracy of the sterile neutrinos, $|M_2 - M_3|/|M_2 + M_3| \sim 10^{-11}$. The required lepton chemical potential is

$$\mu_\alpha \sim 10^{-10} \quad \text{at} \quad T \sim T_{EW} \ . \tag{4.5}$$

At temperatures below T_{EW}, the sphaleron processes are ineffective, so that a change of the lepton chemical potential does not influence the baryon

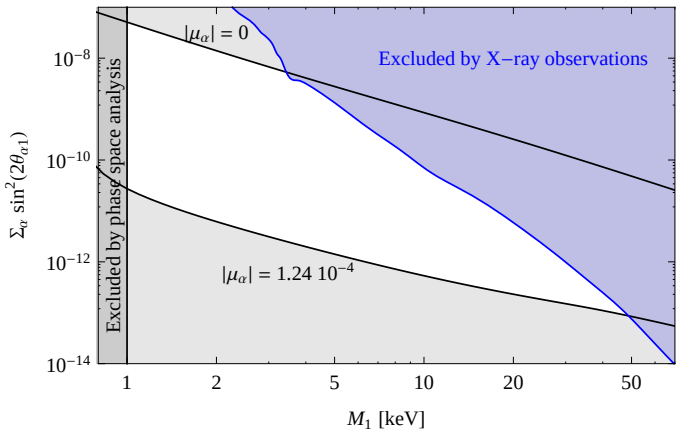

Fig. 8. Constraints on N_1 mass and mixing. The blue region is excluded by X-ray observations, the dark gray region ($M_1 < 1$ keV) by the Tremaine-Gunn bound. On the solid lines the model reproduces the observed value of $\Omega_{\rm DM}$ for the indicated chemical potentials. From Ref. [36].

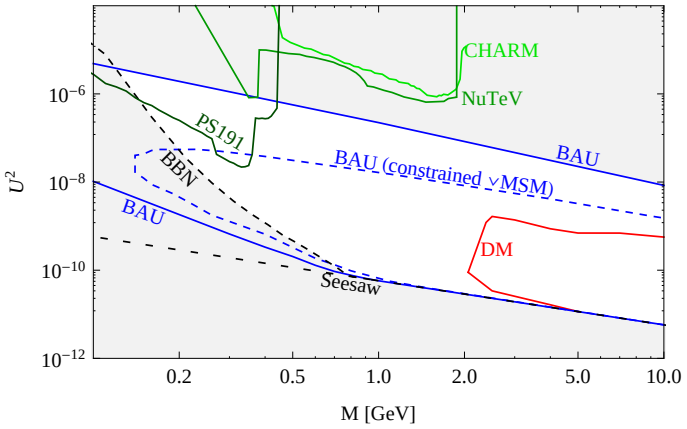

Fig. 9. Experimental and cosmological constraints on mixing $U^2 = {\rm tr}(\theta^\dagger\theta)$ and $N_{2,3}$ masses $M_{2,3} \simeq M$. From Ref. [36].

asymmetry anymore. Now larger lepton chemical potentials are needed to generate the observed amount of dark matter,

$$|\mu_\alpha| \gtrsim 8 \cdot 10^{-6} \quad \text{rm at} \quad T \sim 100 \text{ MeV} \ . \tag{4.6}$$

The observed dark matter abundance $\Omega_{\rm DM}$ also restricts the $N_{2,3}$ masses to lie in the range 2-10 GeV (cf. Fig. 9). Inflation can be incorporated by adding a light dilaton field.

The νMSM scenario requires a reheating temperature $T_R = \mathcal{O}(100\ {\rm GeV})$. It is indeed a minimal model and can be verified or falsified in the near future by astrophysical observations and collider experiments.

5. Example IV: Thermal Leptogenesis

In the previous section we saw that the Standard Model supplemented by three right-handed neutrinos can explain baryogenesis and dark matter for judiciously chosen neutrino masses smaller than the electroweak scale. On the contrary, in the canonical GUT scenario, the sterile neutrinos have GUT scale masses, and the smallness of the light neutrino masses is obtained for Dirac neutrino masses comparable to charged lepton and quark masses. In this case decays of N_1, the lightest of the sterile neutrinos, generate the baryon asymmetry [34]. The mass M_1 of N_1 is much larger than the electroweak scale, and since the N_1 abundance is thermally produced, also the reheating temperature must be much larger than the electroweak scale. Clearly, dark matter is now independent of neutrino physics.

For third generation Yukawa couplings $\mathcal{O}(1)$, as in some SO(10) GUT models, one obtains the heavy and light neutrino masses,

$$M_3 \sim \Lambda_{\rm GUT} \sim 10^{15}\ {\rm GeV}\ , \quad m_3 \sim \frac{v^2}{M_3} \sim 0.01\ {\rm eV}\ . \tag{5.1}$$

Remarkably, the light neutrino mass m_3 is comparable to $(\Delta m^2_{atm})^{1/2} \equiv m_{\rm atm} \simeq 0.05$ eV, as measured in atmospheric ν-oscillations. This supports the hypothesis that neutrino physics probes the mass scale of grand unification.

In the case of hierarchical heavy Majorana neutrinos, the interactions of $N \equiv N_1$, the lightest of them, with the Higgs doublet ϕ and the lepton doublets l_{Li} are described by the effective Lagrangian [38]

$$\begin{aligned}\mathcal{L} \ &= \ \bar{l}_{Li}\widetilde{\phi}\lambda^*_{i1}N + N^T\lambda_{i1}Cl_{Li}\phi - \frac{1}{2}MN^TCN \\ &\quad + \frac{1}{2}\eta_{ij}l^T_{Li}\phi\ Cl_{Lj}\phi + \frac{1}{2}\eta^*_{ij}\bar{l}_{Li}\widetilde{\phi}\ C\bar{l}^T_{Lj}\widetilde{\phi}\ ,\end{aligned} \tag{5.2}$$

where $\widetilde{\phi} = i\sigma_2\phi^*$ and C is the charge conjugation matrix. The quartic coupling

$$\eta_{ij} = \sum_{k>1}\lambda_{ik}\frac{1}{M_k}\lambda^T_{kj} \tag{5.3}$$

is obtained after integrating out heavy Majorana neutrinos $N_{k>1}$ with $M_{k>1} \gg M_1 \equiv M$. Note that in quantum corrections the coupling η takes care of vertex and self-energy contributions. N has small Yukawa couplings, $\lambda_{i1} \ll 1$, and its decay width Γ is therefore much smaller than the mass M.

The heavy Majorana neutrinos have no gauge interactions. Hence, in the early universe, they can easily be out of thermal equilibrium. This makes N, the lightest of them, an ideal candidate for baryogenesis, in accord with Sakharov's condition of departure from thermal equilibrium. In the simplest form of leptogenesis the N abundance is produced by thermal processes, which is therefore called 'thermal leptogenesis'. The *CP*-violating N decays into lepton-Higgs pairs lead to a lepton asymmetry $\langle L\rangle_T \neq 0$, which is partially converted to a baryon asymmetry $\langle B\rangle_T \neq 0$ by the sphaleron processes. In early work on leptogenesis, it was anticipated that the light neutrino masses are then required to have masses $m_i < \mathcal{O}(1\text{eV})$ [39]. After the discovery of atmospheric neutrino oscillations, more stringent upper bounds on neutrino masses could be derived, and leptogenesis became increasingly popular.

The generated baryon asymmetry is proportional to the *CP* asymmetry in N_1 decays. For hierarchical heavy neutrinos it is given by [40–42]

$$\begin{aligned} \epsilon_1 &= \frac{\Gamma(N_1 \to l\phi) - \Gamma(N_1 \to \bar{l}\bar{\phi})}{\Gamma(N_1 \to l\phi) + \Gamma(N_1 \to \bar{l}\bar{\phi})} \\ &= -\frac{3}{16\pi} \frac{\mathrm{Im}(m_D^\dagger m_\nu m_D)_{11} M_1}{\left(m_D^\dagger m_D\right)_{11} v^2} \ . \end{aligned} \tag{5.4}$$

From this expression one obtains the estimate [43]

$$\epsilon_1 \ \sim \ \frac{3}{16\pi} \frac{m_3 M_1}{v^2} \tag{5.5}$$

$$\sim \ 0.1 \ \frac{M_1}{M_3} \ . \tag{5.6}$$

Note that the r.h.s. of Eq. (5.5) is in fact a rigorous upper bound on the *CP* asymmetry ϵ_1 [44, 45]. Using the seesaw formula, Eq. (5.6) relates the *CP* asymmetry to the mass hierarchy of the heavy neutrinos. For mass hierarchies similar to charged lepton and quark mass hierarchies, $M_1/M_3 \sim 10^{-4} \ldots 10^{-5}$, as expected in GUTs, one then obtains the order-of-magnitude estimate $\epsilon_1 \sim 10^{-5} \ldots 10^{-6}$.

The small *CP* asymmetry ϵ_1 in the case of hierarchical heavy neutrinos implies a small baryon asymmetry,

$$\eta_B = \frac{n_B - n_{\bar{B}}}{n_\gamma} = -d \ \epsilon_1 \ \kappa_f \ \sim \ 10^{-9} \ldots 10^{-10} \ . \tag{5.7}$$

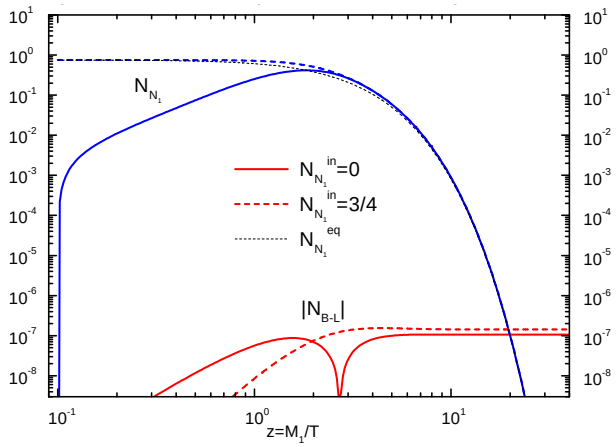

Fig. 10. Evolution of heavy neutrino abundance $\mathrm{N}_{\mathrm{N}_1}$ and lepton asymmetry $\mathrm{N}_{\mathrm{B-L}}$ for typical leptogenesis parameters: $M_1 = 10^{10}$ GeV, $\widetilde{m}_1 = 8\pi\Gamma_1(v_{\mathrm{EW}})/M_1)^2$ eV, $\epsilon_1 = 10^{-6}$; the inverse temperature $z = M_1/T$ is the time variable. The dashed (full) lines correspond to thermal (vacuum) initial conditions for the heavy neutrino abundance; the dotted line represents the equilibrium abundance. From Ref. [47].

Here the dilution factor $d \sim 0.01$ accounts for the increase of the photon number density between leptogenesis and today, and the efficiency factor $\kappa_f \sim 10^{-2}$ is a consequence of washout effects due to lepton number changing scatterings in the plasma.

It turns out that for the relevant range of neutrino masses, the final baryon asymmetry is determined by decays and inverse decays of the heavy neutrinos [46]. In the "one-flavour" approximation, where one sums over lepton flavours in the final state, the Boltzmann equations take the simple form

$$\frac{dn_N}{dt} + 3Hn_N = -\left(n_N - n_N^{eq}\right)\ \Gamma_N\ , \tag{5.8}$$

$$\frac{dn_L}{dt} + 3Hn_L = -\epsilon_1\left(n_N - n_N^{eq}\right)\ \Gamma_N\ . \tag{5.9}$$

Here n_N (n_N^{eq}) and n_L (n_L^{eq}) are the (equilibrium) number densities[2] of heavy neutrinos and leptons, respectively. Note that the *CP* asymmetry ϵ_1 results from a quantum interference. On the contrary, washout terms, which are neglected in Eqs. (5.8) and (5.9), are tree level proesses.

[2] Note that in Fig. 10 number densities $\mathrm{N}_{\mathrm{N}_1}$ and $\mathrm{N}_{\mathrm{B-L}}$ are plotted for a portion of comoving volume that contains one photon.

Solutions of the Boltzmann equations are shown in Fig. 10 for different initial N-distributions: thermal abundance and zero abundance, respectively. It is important that the final $B-L$ asymmetry is essentially independent of the initial conditions. This holds for sufficiently large values of the effective light neutrino mass, $\widetilde{m}_1 \gtrsim 10^{-3}$ eV. In the case of hierarchical GUT scale neutrinos, $M_3 \sim \Lambda_{\rm GUT} \sim 10^{15}$ GeV $\gg M_1 \sim 10^{10}$ GeV, the required reheating temperature is $T_R \sim M_1 \sim 10^{10}$ GeV, eight orders of magnitude larger than the temperature of electroweak baryogenesis.

During the past years detailed studies have been caried out on bounds for neutrino masses and mixings from leptogenesis. It is then important to go beyond the "one-flavour-approximation". Furthermore, important results have been obtained for specific lepton flavour models, in particular in the context of GUT models, for different realizations of the seesaw mechanism, and on the connection with CP violation in low energy processes [48].

6. Cosmological $B-L$ Breaking

So far we have seen that the smallness of the light neutrino masses can be explained by the seesaw mechanism, i.e. their mixing with heavy Majorana neutrinos, and that CP-violating decays and scatterings of these heavy neutrinos naturally yield the observed baryon asymmetry. The heavy Majorana masses break $B-L$, and on theoretical grounds one expects that they result from the spontaneous breaking of a local symmetry. Furthermore, stabilizing the hierarchy between the electroweak scale and the heavy neutrino masses suggests supersymmetry. One thus arrives at a supersymmetric extension of the Standard Model with right-handed neutrinos and local $B-L$ symmetry. It is remarkable that this simple framework contains all the ingredients which are needed to account also for dark matter and inflation, in addition to the matter-antimatter asymmetry. In the following we shall describe this scenario, closely following Ref. [49].

As we have seen in the previous section, thermal leptogenesis requires a rather large reheating temperature, $T_L \sim 10^{10}$ GeV. In supersymmetric theories this causes a potential problem because of gravitino production from the thermal bath [50, 51], which yields the abundance [52, 53],

$$\Omega_{\tilde{G}} h^2 = C \left(\frac{T_R}{10^{10}\,\mathrm{GeV}}\right) \left(\frac{100\,\mathrm{GeV}}{m_{\tilde{G}}}\right) \left(\frac{m_{\tilde{g}}}{1\,\mathrm{TeV}}\right)^2 \ , \tag{6.1}$$

where $C \sim 0.5$, and T_R is the reheating temperature. For unstable gravitinos, one has to worry about consistency with primordial nucleosynthesis (BBN) whereas stable gravitinos may overclose the universe. As a possible way out, nonthermal production of heavy neutrinos has been suggested [54–57], which allows to decrease the reheating temperature and

therefore the gravitino production. On the other hand, it is remarkable that for typical gravitino and gluino masses in gravity mediated supersymmetry breaking, a reheating temperature $T_R \sim 10^{10}\,\mathrm{GeV}$ yields the right order of magnitude for the dark matter abundance if the gravitino is the LSP. But why should the reheating temperature be as large as the temperature favoured by leptogenesis, i.e., $T_R \sim T_L$?

It this context it is interesting to note that for typical neutrino mass parameters in leptogenesis, $\widetilde{m}_1 \sim 0.01\,\mathrm{eV}$, $M_1 \sim 10^{10}\,\mathrm{GeV}$, the heavy neutrino decay width takes the value

$$\Gamma^0_{N_1} = \frac{\widetilde{m}_1}{8\pi}\left(\frac{M_1}{v_{\mathrm{EW}}}\right)^2 \sim 10^3\ \mathrm{GeV}\ . \tag{6.2}$$

If the early universe in its evolution would reach a state where the energy density is dominated by nonrelativistic heavy neutrinos, their subsequent decays to lepton-Higgs pairs would then yield a relativistic plasma with temperature

$$T_{\mathrm{R}} \sim 0.2 \cdot \sqrt{\Gamma^0_{N_1} M_P} \sim 10^{10}\ \mathrm{GeV}\ , \tag{6.3}$$

which is indeed the temperature wanted for gravitino dark matter! Is this an intriguing hint or just a misleading coincidence?

6.1. B−L Breaking and False Vacuum Decay

We shall now demonstrate that an intermediate stage of heavy neutrino dominance indeed occurs in the course of the cosmological evolution if the initial inflationary phase is driven by the false vacuum energy of unbroken B-L symmetry [49, 58].

Consider the supersymmetric standard model with right-handed neutrinos, described by the superpotential (in $SU(5)$ notation: $\mathbf{10} = (q, u^c, e^c)$, $\mathbf{5}^* = (d^c, l)$),

$$\begin{aligned} W_M = {} & h^u_{ij}\mathbf{10}_i\mathbf{10}_j H_u + h^d_{ij}\mathbf{5}^*_i\mathbf{10}_j H_d \\ & + h^\nu_{ij}\mathbf{5}^*_i n^c_j H_u + h^n_i n^c_i n^c_i S_1\ , \end{aligned} \tag{6.4}$$

supplemented by a term which enforces B-L breaking,

$$W_{B-L} = \frac{\sqrt{\lambda}}{2}\Phi\left(v^2_{B-L} - 2S_1S_2\right)\ . \tag{6.5}$$

The Higgs fields $H_{u,d}$ and $S_{1,2}$ break electroweak symmetry and B-L symmetry, respectively, with $\langle H_{u,d}\rangle = v_{u,d}$ and $\langle S_{1,2}\rangle = v_{B-L}/\sqrt{2}$. It is well known that the superpotential W_{B-L} can successfully describe inflation with Φ as inflaton field, which is referred to as F-term hybrid inflation [59, 60].

ψ_i	$\mathbf{10}_3$	$\mathbf{10}_2$	$\mathbf{10}_1$	$\mathbf{5}^*_{3,2}$	$\mathbf{5}^*_1$	$n^c_{3,2}$	n^c_1	$H_{u,d}$	$S_{1,2}$	Φ
Q_i	0	1	2	a	$a+1$	$d-1$	d	0	0	$2(d-1)$

Table 2. Assignement of FN charges of $U(1)$ flavour symmetry.

The Yukawa couplings in the superpotential W_M are largely determined by low energy physics of quarks, charged leptons and neutrinos. It is useful to take this into account by means of a specific flavour model. In the following we choose a model with $U(1)$ flavour symmetry of Froggatt-Nielsen (FN) type. Up to factors $\mathcal{O}(1)$, the Yukawa couplings are given by

$$h_{ij} \sim \eta^{Q_i+Q_j} \ , \quad \sqrt{\lambda} \sim \eta^{Q_\Phi} \ , \tag{6.6}$$

with $\eta \simeq 1/\sqrt{300}$. The FN charges Q_i are chosen following Ref. [43] and listed in Table 2.

For simplicity, we will restrict our analysis to the case of a hierarchical heavy (s)neutrino mass spectrum, $M_1 \ll M_2, M_3$, where $M = h^n\, v_{B-L}$. Furthermore, we assume the heavier (s)neutrino masses to be of the same order of magnitude as the common mass m_S of the particles in the symmetry breaking sector, for definiteness we set $M_2 = M_3 = m_S$. Taking the $B-L$ gauge coupling to be $g^2 = g^2_{GUT} \simeq \pi/6$, the model is, up to $\mathcal{O}(1)$ factors, determined by the $U(1)_{\rm FN}$ charges a and d. The $B-L$ breaking scale v_{B-L}, the mass of the lightest of the heavy (s)neutrinos M_1, and the effective light neutrino mass parameter $\widetilde{m}_1$ are related to these by

$$v_{B-L} \sim \eta^{2a} \frac{v^2_{\rm EW}}{\overline{m}_\nu} \ , \quad M_1 \sim \eta^{2d} v_{B-L} \ , \tag{6.7}$$

$$\widetilde{m}_1 = \frac{(m_D^\dagger m_D)_{11}}{M_1} \sim \eta^{2a} \frac{v^2_{\rm EW}}{v_{B-L}} \ , \tag{6.8}$$

where $\overline{m}_\nu = \sqrt{m_2 m_3}$, the geometric mean of the two light neutrino mass eigenvalues m_2 and m_3, characterizes the light neutrino mass scale that, with the charge assignments above, can be fixed to 3×10^{-2} eV. Here, the seesaw formula $m_\nu = -m_D M^{-1} m_D^T$ has been exploited, with $m_D = h^\nu v_{\rm EW}$. Note, that $\widetilde{m}_1$ is bounded from below by the lightest neutrino mass m_1 [61]. Instead of the FN $U(1)$ flavour charges the physical quantities v_{B-L}, M_1 and $\widetilde{m}_1$ can be used as parameters of the model. In the discussion of dark matter the gravitino ($m_{\tilde{G}}$) and gluino ($m_{\tilde{g}}$) masses enter as additional parameters.

Before the spontaneous breaking of $B-L$, supersymmetry is broken by the vacuum energy density $\rho_0 = \frac{1}{4}\lambda v^4_{B-L}$, which drives inflation. During this time, the dynamics of the system is governed by the slowly rolling scalar component ϕ of the inflaton multiplet Φ. The scalar components of

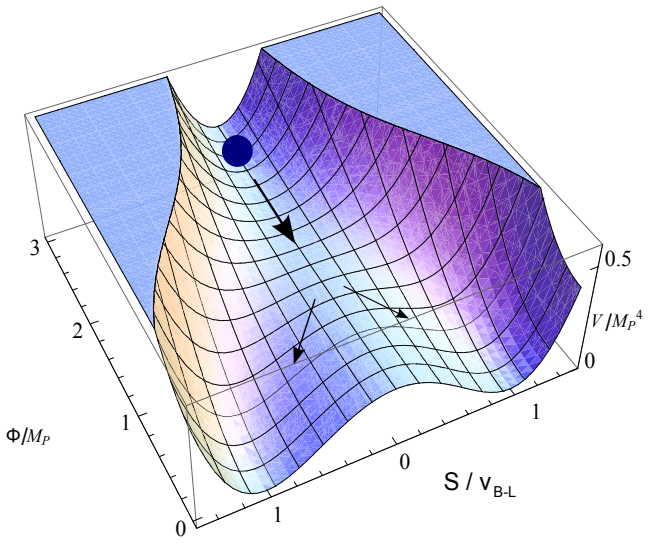

Fig. 11. Hybrid inflation: The time evolution of the inflaton field Φ leads to a tachyonic mass of the waterfall field S, which triggers a rapid transition to a phase with spontaneously broken $B-L$ symmetry.

the Higgs superfields $S_{1,2}$ are stabilized at zero. As the field value of the inflaton decreases, so do the effective masses in the Higgs sector, until a tachyonic direction develops in the effective scalar potential, which triggers a rapid transition to a phase with spontaneously broken $B-L$ aymmetry (see Fig. 11).

The phase transition is best treated in unitary gauge where the physical degrees of freedom are manifest. Performing a super-gauge transformation relates the Higgs superfields $S_{1,2}$ and the vector superfield V to the respective fields S' and Z in unitary gauge,

$$S_{1,2} = \frac{1}{\sqrt{2}}\, S' \, \exp(\pm iT)\,, \qquad V = Z + \frac{i}{2gq_S}(T - T^*)\,. \tag{6.9}$$

The supermultiplet S' contains two real scalar degrees of freedom, $s' = \frac{1}{\sqrt{2}}(\sigma' + i\tau)$, where τ remains massive throughout the phase transition and σ' is the symmetry breaking Higgs field. It acquires a vacuum expectation value proportional to $v(t) = \frac{1}{\sqrt{2}}\langle \sigma'^2(t,\vec{x})\rangle_{\vec{x}}^{1/2}$ which approaches v_{B-L} at large times. In the Lagrangian, symmetry breaking is described by the replacement $\sigma' \to \sqrt{2}v(t)+\sigma$, where σ denotes the fluctuations around the homogeneous Higgs background. The fermionic component $\tilde{s}$ of the supermultiplet S' pairs up with the fermionic component $\tilde{\phi}$ of the inflaton supermultiplet Φ

to form a Dirac fermion ψ, the higgsino, which becomes massive during the phase transition. Due to supersymmetry, the corresponding scalar fields (σ, τ and inflaton ϕ) have the same mass as the higgsino in the supersymmetric true vacuum. Likewise, the gauge supermultiplet Z (gauge boson A, real scalar C, Dirac gaugino $\tilde{A}$) and the (s)neutrinos N_i ($\tilde{N}_i$) acquire masses.

At the end of the phase transition, supersymmetry is restored. An explicit calculation of the Lagrangian describing this phase transition yields the time-dependent mass eigenvalues:

$$\begin{aligned} &m_\sigma^2 = \frac{1}{2}\lambda(3v^2(t) - v_{B-L}^2)\,, \qquad m_\tau^2 = \frac{1}{2}\lambda(v_{B-L}^2 + v^2(t))\ , \\ &m_\phi^2 = \lambda v^2(t)\,, \qquad m_\psi^2 = \lambda v^2(t)\,, \\ &m_Z^2 = 8g^2v^2(t)\ , \\ &M_i^2 = (h_i^n)^2 v^2(t)\ , \end{aligned} \tag{6.10}$$

where we corrections due to thermal effects and supersymmetry breaking have been ignored.

The symmetry breaking proceeds very rapidly, and therefore it is often referred to as a 'waterfall' transition. It is accompanied by the production of local topological defects in the form of cosmic strings as well as the nonadiabatic production of particles coupled to the Higgs field, a process commonly known as tachyonic preheating [62].

The cosmic strings produced during the phase transition have an energy per unit length [63],

$$\mu = 2\pi B(\beta) v_{B-L}^2\,, \tag{6.11}$$

with $\beta = \lambda/(8\,g^2)$ and $B(\beta) = 2.4\,[\ln(2/\beta)]^{-1}$ for $\beta < 10^{-2}$. According to Ref. [64], the characteristic length separating two strings formed during tachyonic preheating is

$$\xi = (-\lambda v_{B-L}\dot{\varphi}_c)^{-1/3}\,. \tag{6.12}$$

Here $\dot{\varphi}_c$ is the velocity of the radial component of the inflaton field, $\phi = \varphi/\sqrt{2}e^{i\theta}$, at the onset of the phase transition, which can be determined from the scalar potential using the equation of motion for φ. In the region of parameter space we are interested in, the slope of the scalar potential is determined by the one-loop quantum corrections (cf., e.g., Ref. [65]). With this, one obtains for the energy density stored in strings just after the end of the phase transition

$$\rho_{\text{string}} = \frac{\mu}{\xi^2}\ . \tag{6.13}$$

From Eqs. (6.11), (6.12) and the one-loop potential, one finds that the fraction of energy stored in cosmic strings directly after the phase transition

increases strongly with the coupling λ. This is due to the higher energy density per cosmic string as well as the shorter average distance between two strings. For instance, for $v_{B-L} = 5 \times 10^{15}$ GeV and $\lambda = 10^{-2}$, one has $(H\xi)^{-1} \simeq 400$ and $\rho_{\rm string}/\rho_0 \simeq 60\,\%$. For $\lambda = 10^{-5}$, this is reduced to $(H\xi)^{-1} \simeq 40$ and $\rho_{\rm string}/\rho_0 \simeq 0.2\,\%$.

These relic cosmic strings can in principal be observed today, e.g. via string induced gravitational lensing effects in the CMB. The nonobservation of these effects implies an upper bound on the energy per unit length [66–68],

$$G\mu \lesssim 5 \times 10^{-7}\,, \tag{6.14}$$

where $G = {M_{\rm P}}^{-2}$ is Newton's constant with $M_{\rm P} = 1.22 \times 10^{19}$ GeV denoting the Planck mass. Inserting this into Eq. (6.11) puts an upper bound on v_{B-L}. In Ref. [65], also the bounds inferred from the spectrum of fluctuations in the CMB [69] have been taken into account, yielding the viable parameter range

$$\begin{aligned} &3 \times 10^{15}\ \text{GeV} \lesssim v_{B-L} \lesssim\ 7 \times 10^{15}\ \text{GeV}\,, \\ &10^{-4} \lesssim \sqrt{\lambda} \lesssim\ 10^{-1}\,. \end{aligned} \tag{6.15}$$

This significantly constrains the model parameters. With the scale of $B-L$ breaking basically fixed, one finds for the FN flavour charges $a = 0$ and $1.4 \lesssim d \lesssim 2.6$, corresponding to the range

$$\begin{aligned} &10^{9}\ \text{GeV} \leq M_1 \leq 3 \times 10^{12}\ \text{GeV}\ , \\ &10^{-5}\ \text{eV} \leq \widetilde{m}_1 \leq 1\ \text{eV}\ . \end{aligned} \tag{6.16}$$

During tachyonic preheating, quantum fluctuations of the Higgs field σ_k' with wave number $|\vec{k}| < |m_\sigma|$ grow exponentially, while its average value remains zero. The strong population of the long wavelength Higgs modes leads to a large abundance of nonrelativistic Higgs bosons. Other particles coupled to the Higgs field are nonperturbatively produced due to the rapid change of their effective masses [70].

The mode equations for the gauge, Higgs, inflaton, and neutrino supermultiplets are governed by the time-dependent masses proportional to $v(t)$ listed in Eq. (6.10). This leads to particle production [70], with number densities for bosons and fermions after tachyonic preheating given by[3]

$$\begin{aligned} n_B(\alpha) &\simeq 1 \times 10^{-3} g_s m_S^3 f(\alpha, 1.3)/\alpha\ , \\ n_F(\alpha) &\simeq 3.6 \times 10^{-4} g_s m_S^3 f(\alpha, 0.8)/\alpha\ , \end{aligned} \tag{6.17}$$

[3] Note that particle production can be significantly enhanced by quantum effects [71], which require further investigations.

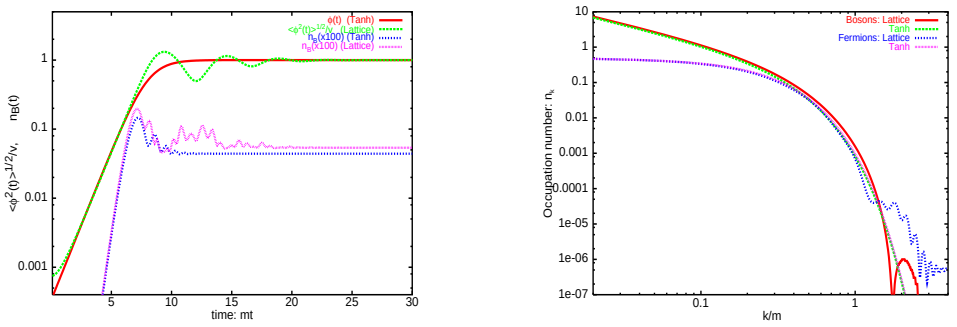

Fig. 12. (a) (left) Growth of the $B-L$ Higgs expectation value as function of time. (b) (right) Occupation numbers of bosons and fermions produced during tachyonic preheating as functions of momentum. From Ref. [70].

with $f(\alpha,\gamma)=\sqrt{\alpha^2+\gamma^2}-\gamma$ and $\alpha=m_X/m_S$, where m_X denotes the mass of the respective particle in the true vacuum; g_s counts the spin degrees of freedom of the respective particle. Just as the Higgs bosons themselves, these particles are produced with very low momenta, i.e. nonrelativistically.

6.2. The Reheating Process

During tachyonic preheating, most of the vacuum energy is converted into Higgs bosons (σ). At the same time, particles coupled to the Higgs field, i.e. quanta of the gauge, Higgs, inflaton and neutrino supermultiplets are produced, with the resulting abundances given by Eq. (6.17). Among these particles, the members of the gauge supermultiplet have by far the shortest lifetime. Due to their large couplings they decay basically instantaneously into (s)neutrinos and MSSM particles. This sets the initial conditions for the following phase of reheating, which can be described by means of Boltzmann equations.

Due to the choice of the hierarchical (s)neutrino mass spectrum, the decay of particles from the symmetry breaking sector into the two heavier (s)neutrino generations is kinematically forbidden. These particles can hence only decay into particles of the N_1 supermultiplet. These (s)neutrinos, just as the neutrinos produced through gauge particle decays and thermally produced (s)neutrinos, decay into MSSM particles, thereby generating the entropy of the thermal bath as well as a lepton asymmetry. Note that these different production mechanisms for the (s)neutrinos yield (s)neutrinos with different energies, which due to relativistic time-dilatation, decay at differ-

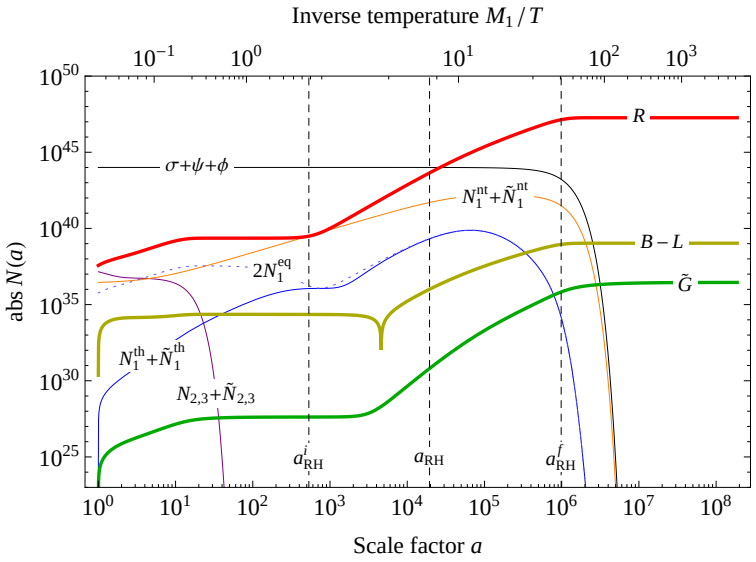

Fig. 13. Comoving number densities for particles from the symmetry breaking sector (Higgs σ + higgsinos ψ + inflatons ϕ), (non)thermally produced (s)neutrinos of the first generation ($N_1^{\rm th}+\tilde{N}_1^{\rm th}$, $N_1^{\rm nt}+\tilde{N}_1^{\rm nt}$), (s)neutrinos of the first generation in thermal equilibrium ($2N_1^{\rm eq}$, for comparison), (s)neutrinos of the second and third generation ($N_{2,3}+\tilde{N}_{2,3}$), the MSSM radiation (R), the lepton asymmetry ($B-L$), and gravitinos ($\widetilde{G}$) as functions of the scale factor a. The vertical lines labeled $a_{\rm RH}^i$, $a_{\rm RH}$ and $a_{\rm RH}^f$ mark the beginning, the middle and the end of the reheating process. From Ref. [49].

ent rates. Finally, the thermal bath produces a thermal gravitino density, which turns out to be in the right ball-park to yield the observed dark matter abundance.

The network of Boltzmann equations for the time evolution of all particles and superparticles is described in detail in Ref. [49]. Their solution provides the initial conditions of the hot early universe. In Fig. 13 the result is shown for an illustrative choice of parameters,

$$\begin{aligned} M_1 &= 5.4\times 10^{10}\,\text{GeV}\ , \quad \widetilde{m}_1 = 4.0\times 10^{-2}\,\text{eV}\ , \\ m_{\widetilde{G}} &= 100\,\text{GeV}\ , \quad m_{\tilde{g}} = 1\,\text{TeV}\ . \end{aligned} \tag{6.18}$$

Due to the rapid decay of gauge particles, the total energy density has already right after the end of tachyonic preheating a small relativistic component. For a rather long period, during which the scale factor grows by six orders of magnitude, it is dominated by the nonrelativistiv gas of Higgs

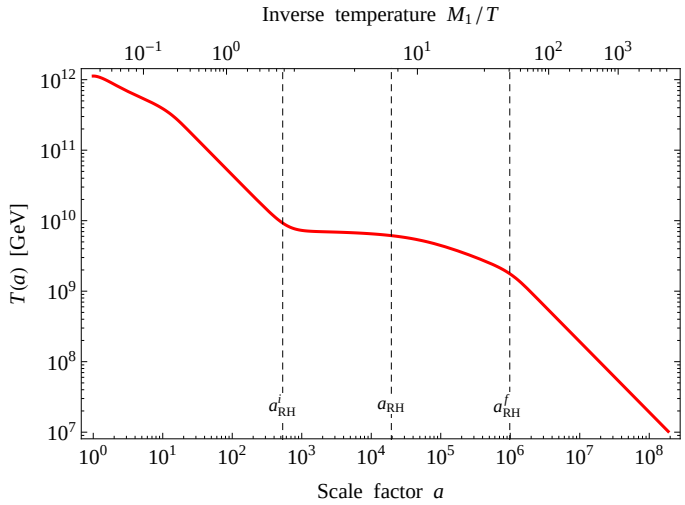

Fig. 14. Temperature T of the thermal bath as function of the scale factor a. From Ref. [49].

bosons. Their decay via heavy neutrinos then generates the bulk of entropy, baryon asymmetry and gravitino abundance. For the chosen parameters, dark matter is made of gravitinos. Their abundance and the baryon-to-photon ratio are consistent with observation,

$$\eta_B \simeq 3.7 \times 10^{-9} \ , \quad \Omega_{\widetilde{G}} h^2 \simeq 0.11 \ . \tag{6.19}$$

Note that the given baryon-to-photon ratio corresponds to maximal *CP* asymmetry, which can be reduced by an appropriate choice of phases in the neutrino mass matrices.

A key feature of the described reheating process is the emergence of an approximate temperature plateau between $a^i_{\rm RH}$ and $a^f_{\rm RH}$. The corresponding temperature $T_R \equiv T(a_{\rm RH})$ is determined by neutrino masses,

$$T_R \simeq 1.3 \times 10^{10}\,{\rm GeV} \left(\frac{\widetilde{m}_1}{0.04\,{\rm eV}}\right)^{1/4} \left(\frac{M_1}{10^{11}\,{\rm GeV}}\right)^{5/4} \ . \tag{6.20}$$

The temperature plateau occurs as result of a competition between universe expansion and entropy production in N_1 decays. During this period most of the baryon asymmetry and dark matter are produced.

6.3. Leptogenesis and Dark Matter

In the described reheating process, baryogenesis is a mixture of non-thermal and thermal leptogenesis, which considerably extends the viable

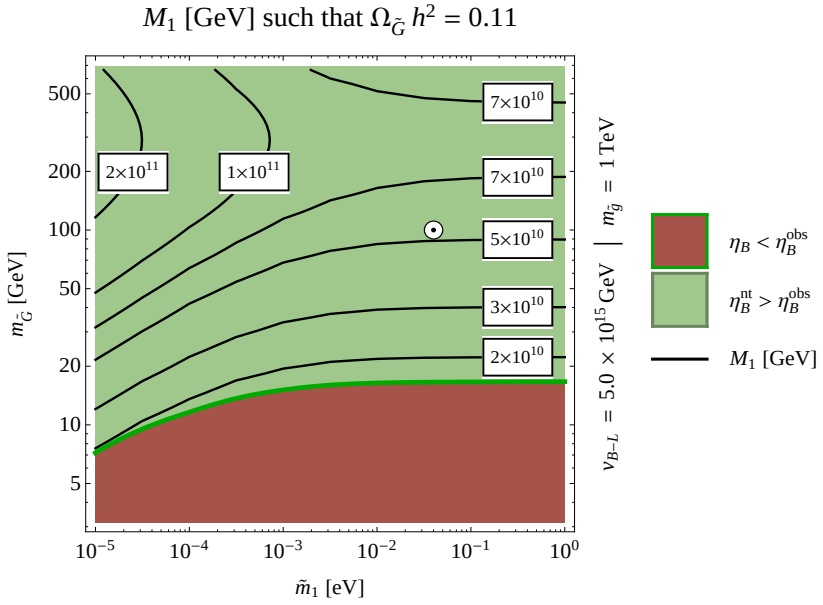

Fig. 15. Contour plots of the heavy neutrino mass M_1 as function of the effective neutrino mass $\widetilde{m}_1$ and the gravitino mass $m_{\widetilde{G}}$ such that the relic density of dark matter is accounted for by gravitinos. In the red region the lepton asymmetry generated by leptogenesis is smaller than the observed one, providing a lower bound on the gravitino mass, depending on $\widetilde{m}_1$. From Ref. [49].

range in the $M_1 - \widetilde{m}_1$ plane compared to thermal leptogenesis. Gravitino production is dominated by thermal processes. A systematic parameter scan shows that gravitino dark matter is possible in the mass range 10 GeV $\lesssim m_{\widetilde{G}} \lesssim$ 700 GeV (assuming $m_{\widetilde{g}} \simeq 1$ TeV) (cf. Fig. 15). Gravitino dark matter further constrains the heavy neutrino mass to the range 2×10^{10} GeV $\lesssim M_1 \lesssim 2 \times 10^{11}$ GeV, which is more stringent than the constraint from inflation.

Recent results on the Higgs boson mass from the LHC motivate a superparticle mass spectrum with a very heavy gravitino [72, 73],

$$m_{\rm LSP} \ll m_{\rm squark,slepton} \ll m_{\widetilde{G}} \; . \tag{6.21}$$

Due to this hierarchy the LSP is typically a 'pure' gaugino or higgsino. A pure neutral wino or higgsino is almost mass degenerate with a chargino belonging to the same SU(2) multiplet. Hence, the current lower bound on chargino masses also applies to the LSP, $m_{\rm LSP} \geq 94$ GeV [32]. It is well known that a gravitino heavier than 10 TeV can be consistent with

primordial nucleosynthesis as well as leptogenesis [74, 75].

The thermal abundance of a pure wino ($\widetilde{w}$) or higgsino ($\widetilde{h}$) LSP becomes significant for masses above 1 TeV, where it is well approximated by [76–78]

$$\Omega^{\rm th}_{\widetilde{w},\widetilde{h}}h^2 = c_{\widetilde{w},\widetilde{h}}\left(\frac{m_{\widetilde{w},\widetilde{h}}}{1\ {\rm TeV}}\right)^2 , \quad c_{\widetilde{w}} = 0.014 , \quad c_{\widetilde{h}} = 0.10 , \tag{6.22}$$

for wino and higgsino, respectively.

Consider now gravitino masses in the range from 10 TeV to 10^3 TeV. The gravitino lifetime is given by

$$\tau_{\widetilde{G}} = \left(\frac{1}{32\pi}\left(n_v + \frac{n_m}{12}\right)\frac{m^3_{\widetilde{G}}}{M_{\rm P}^2}\right)^{-1} = 24\left(\frac{10\ {\rm TeV}}{m_{\widetilde{G}}}\right)^3 {\rm s} , \tag{6.23}$$

where $n_v = 12$ and $n_m = 49$ are the number of vector and chiral matter multiplets in the MSSM, respectively. The lifetime (6.23) corresponds to the decay temperature

$$T_{\widetilde{G}} = \left(\frac{90\ M_{\rm P}^2}{\pi^2 g_*(T_{\widetilde{G}})\tau^2_{\widetilde{G}}}\right)^{1/4} = 0.24\left(\frac{10.75}{g_*(T_{\widetilde{G}})}\right)^{1/4}\left(\frac{m_{\widetilde{G}}}{10\ {\rm TeV}}\right)^{3/2}{\rm MeV} , \tag{6.24}$$

with $g_*(T_{\widetilde{G}}) = 43/4$ counting the effective number of relativistic degrees of freedom. For gravitino masses between 10 TeV to 10^3 TeV the decay temperature $T_{\widetilde{G}}$ varies between 0.2 MeV and 200 MeV, i.e. roughly between the temperatures of nucleosynthesis and the QCD phase transition. In this temperature range the entropy increase due to gravitino decays and hence the corresponding dilution of the baryon asymmetry are negligible.

The decay of a heavy gravitino, $m_{\widetilde{G}} \gg m_{\rm LSP}$, produces approximately one LSP. This yields the nonthermal contribution to dark matter [80]

$$\Omega^{\widetilde{G}}_{\rm LSP}h^2 = \frac{m_{\rm LSP}}{m_{\widetilde{G}}}\Omega_{\widetilde{G}}h^2 \simeq 2.7\times 10^{-2}\left(\frac{m_{\rm LSP}}{100\ {\rm GeV}}\right)\left(\frac{T_R(M_1,\widetilde{m}_1)}{10^{10}\ {\rm GeV}}\right) , \tag{6.25}$$

where the reheating temperature is given by Eq. (6.20). For LSP masses below 1 TeV, which are most interesting for the LHC as well as for direct searches, the total LSP abundance

$$\Omega_{\widetilde{w},\widetilde{h}}h^2 = \Omega^{\widetilde{G}}_{\widetilde{w},\widetilde{h}}h^2 + \Omega^{\rm th}_{\widetilde{w},\widetilde{h}}h^2 \tag{6.26}$$

is thus dominated by the contribution from gravitino decays.

The requirement of higgsino/wino dark matter, i.e. $\Omega_{\rm LSP}h^2 = \Omega_{\rm DM}h^2 \simeq 0.11$, implies an upper bound on the reheating temperature, $T_R < 4.2\times$

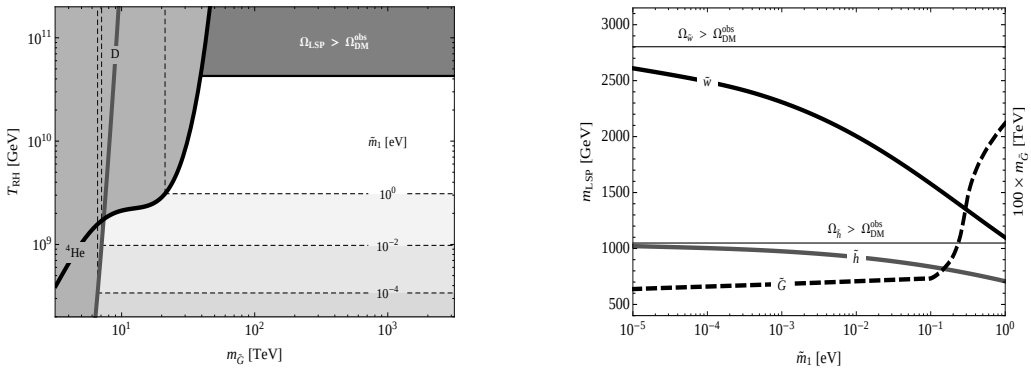

Fig. 16. (a) (left) Upper and lower bounds on the reheating temperature as functions of the gravitino mass. The horizontal dashed lines denote lower bounds imposed by leptogenesis for different values of the effective neutrino mass $\widetilde{m}_1$; the curves labelled ^{4}He and D denote upper bounds originating from the primordial helium-4 and deuterium abundances created during BBN [79]. The shaded region marked $\Omega_{\rm LSP} > \Omega_{\rm DM}^{\rm obs}$ is excluded by overproduction of dark matter. (b) (right) Upper bounds on wino ($\widetilde{w}$) and higgsino ($\widetilde{h}$) LSP masses imposed by successful leptogenesis as well as absolute lower bound on the gravitino mass according to BBN as functions of the effective neutrino mass $\widetilde{m}_1$. From Ref. [80].

10^{10} GeV. A lower bound on T_R is obtained from leptogenesis, depending on $\widetilde{m}_1$ (cf. Fig. 16(a)). Higgsino/wino dark matter also implies an upper bound on the LSP mass, depending on $\widetilde{m}_1$, and a lower bound on the gravitino mass (cf. Fig. 16(b)). For instance, for $m_1 = 0.05$ eV, one has $m_{\widetilde{h}} \lesssim 900$ GeV, $m_{\widetilde{G}} \gtrsim 10$ TeV.

In summary, in the described scenario of cosmological $B-L$ breaking, the reheating temperature can vary in the range 3×10^8 GeV $\lesssim T_R \lesssim 5 \times 10^{10}$ GeV, depending on the nature of dark matter, i.e. gravitino or higgsino/wino.

7. Conclusions and Outlook

In the previous sections we have discussed several mechanisms for the generation of matter and dark matter, which differ significantly with respect to the theoretical framework, the predictive power and the required reheating temperature in the early universe:

- $T_R = \mathcal{O}(100$ MeV): A reheating temperature just above the temperature where nucleosynthesis starts, is sufficient to generate baryon

asymmetry and dark matter in moduli decay. The existence of such scalar fields is a generic feature of string compactifications. The model predicts nonthermal WIMP dark matter. The values of baryon asymmetry and dark matter abundance cannot be predicted since they depend on unknown moduli couplings.

- $T_R = \mathcal{O}(100\ \text{GeV})$: Electroweak baryogenesis is a generic prediction of the Standard Model, which makes use of the electroweak phase transition and sphaleron processes in the high-temperature phase. However, due to the rather large Higgs mass realized in nature, electroweak baryogenesis does not work in the Standard Model, not even in its supersymmetric extension. It remains a viable option in case of a strongly interacting Higgs sector, which will be tested at the LHC.

- $T_R = \mathcal{O}(100\ \text{GeV})$: The νMSM is indeed the most minimal extension of the Standard Model, which can account for both, baryogenesis and dark matter. However, a judicious choice of neutrino masses and mixings is required, which appears difficult to justify theoretically. The model can be verified or falsified by collider experiments and astrophysical observations in the near future.

- $T_R = \mathcal{O}(10^{10}\ \text{GeV})$: Thermal leptogensis in its simplest version explains the baryon asymmetry in terms of neutrino masses and mixings that are consistent with GUT model building. Dark matter must have another origin. Standard WIMP dark matter is incompatible with thermal leptogenesis.

Finally, we have described how spontaneous $B-L$ breaking together with supersymmetry can account for baryon asymmetry, dark matter and inflation. The reheating temperature T_R can vary from $\mathcal{O}(10^8\text{GeV})$ to $\mathcal{O}(10^{11}\text{GeV})$. This simple picture is naturally consistent with neutrino physics and GUT models. During the coming years we can hope to learn from LHC data and astrophysical observations whether matter and dark matter are remnants of the very early universe at temperatures $\mathcal{O}(100\ \text{GeV})$, or whether temperatures several orders of magnitude larger are needed, a possibility that is favoured by the idea of grand unification.

Acknowledgments

The author thanks the organizers for their hospitality, Valerie Domcke and Kai Schmitz for enjoyable collaboration on the topic of these lectures, and Thomas Konstandin for comments on the manuscript. This work has been supported by the German Science Foundation (DFG) within the Collaborative Research Center 676 “Particles, Strings and the Early Universe”.

REFERENCES

[1] For detailed discussions and references see, for example,
V. Mukhanov, "Physical foundations of cosmology," Cambridge, UK: Univ. Pr. (2005) 421 p;
D. S. Gorbunov and V. A. Rubakov, Hackensack, USA: World Scientific (2011) 473 p.

[2] S. Kachru, R. Kallosh, A. D. Linde and S. P. Trivedi, Phys. Rev. D **68** (2003) 046005 [hep-th/0301240].

[3] W. Buchmuller, K. Hamaguchi, O. Lebedev and M. Ratz, Nucl. Phys. B **699** (2004) 292 [hep-th/0404168]; JCAP **0501** (2005) 004 [hep-th/0411109].

[4] K. Schmitz, DESY-THESIS-2012-039.

[5] K. Nakayama, S. Saito, Y. Suwa and J. 'i. Yokoyama, JCAP **0806** (2008) 020 [0804.1827 [astro-ph]].

[6] R. Kitano, H. Murayama and M. Ratz, Phys. Lett. B **669** (2008) 145 [0807.4313 [hep-ph]].

[7] L. Randall and R. Sundrum, Nucl. Phys. B **557** (1999) 79 [hep-th/9810155].

[8] G. F. Giudice, M. A. Luty, H. Murayama and R. Rattazzi, JHEP **9812** (1998) 027 [hep-ph/9810442].

[9] A. D. Sakharov, [JETP Lett. **5** (1967) 24]

[10] E. W. Kolb and M. S. Turner, *The Early Universe* (Addison Wesley, New York, 1990).

[11] Z. Fodor, J. Hein, K. Jansen, A. Jaster and I. Montvay, Nucl. Phys. B **439** (1995) 147 [hep-lat/9409017].

[12] K. Kajantie, M. Laine, K. Rummukainen and M. E. Shaposhnikov, Nucl. Phys. B **466** (1996) 189 [hep-lat/9510020].

[13] W. Buchmuller, Z. Fodor and A. Hebecker, Nucl. Phys. B **447** (1995) 317 [hep-ph/9502321].

[14] K. Jansen, Nucl. Phys. Proc. Suppl. **47** (1996) 196 [hep-lat/9509018].

[15] W. Buchmuller and O. Philipsen, Nucl. Phys. B **443** (1995) 47 [hep-ph/9411334].

[16] K. Kajantie, M. Laine, K. Rummukainen and M. E. Shaposhnikov, Phys. Rev. Lett. **77** (1996) 2887 [hep-ph/9605288].

[17] F. Csikor, Z. Fodor and J. Heitger, Nucl. Phys. Proc. Suppl. **73** (1999) 659 [hep-ph/9809293].

[18] Z. Fodor, Nucl. Phys. Proc. Suppl. **83** (2000) 121 [hep-lat/9909162].

[19] F. Eberlein, Nucl. Phys. B **550** (1999) 303 [hep-ph/9811513].

[20] D. Bieletzki, K. Lessmeier, O. Philipsen and Y. Schroder, JHEP **1205** (2012) 058 [1203.6538 [hep-ph]].

[21] W. Buchmuller and O. Philipsen, Phys. Lett. B **397** (1997) 112 [hep-ph/9612286].

[22] G. Aad *et al.* [ATLAS Collaboration], Phys. Lett. B **716** (2012) 1 [1207.7214 [hep-ex]]; S. Chatrchyan *et al.* [CMS Collaboration], Phys. Lett. B **716** (2012) 30 [1207.7235 [hep-ex]].

[23] G. 't Hooft, Phys. Rev. Lett. **37** (1976) 8.

[24] V. A. Kuzmin, V. A. Rubakov and M. E. Shaposhnikov, Phys. Lett. B **155** (1985) 36.

[25] D. Bodeker, G. D. Moore and K. Rummukainen, Phys. Rev. D **61** (2000) 056003 [hep-ph/9907545].

[26] D. E. Kharzeev, L. D. McLerran and H. J. Warringa, Nucl. Phys. A **803** (2008) 227 [0711.0950 [hep-ph]].

[27] T. Kalaydzhyan and I. Kirsch, Phys. Rev. Lett. **106** (2011) 211601 [1102.4334 [hep-th]].

[28] J. A. Harvey and M. S. Turner, Phys. Rev. D **42** (1990) 3344.

[29] J. R. Espinosa, T. Konstandin and F. Riva, Nucl. Phys. B **854** (2012) 592 [1107.5441 [hep-ph]].

[30] J. R. Espinosa, B. Gripaios, T. Konstandin and F. Riva, JCAP **1201** (2012) 012 [1110.2876 [hep-ph]].

[31] For a review and references see, for example,
W. Bernreuther, "CP violation and baryogenesis," Lect. Notes Phys. **591** (2002) 237 [hep-ph/0205279]; J. M. Cline, "Baryogenesis," hep-ph/0609145.

[32] J. Beringer *et al.* [Particle Data Group Collaboration], Phys. Rev. D **86** (2012) 010001.

[33] M. Carena, G. Nardini, M. Quiros and C. E. M. Wagner, 1207.6330 [hep-ph].

[34] M. Fukugita and T. Yanagida, Phys. Lett. B **174** (1986) 45.

[35] T. Asaka, S. Blanchet and M. Shaposhnikov, Phys. Lett. B **631** (2005) 151 [hep-ph/0503065]; Phys. Lett. B **620** (2005) 17 [hep-ph/0505013].

[36] L. Canetti, M. Drewes and M. Shaposhnikov, 1204.3902 [hep-ph]; L. Canetti, M. Drewes, T. Frossard and M. Shaposhnikov, 1208.4607 [hep-ph].

[37] E. K. Akhmedov, V. A. Rubakov and A. Y. .Smirnov, Phys. Rev. Lett. **81** (1998) 1359 [hep-ph/9803255].

[38] W. Buchmuller and S. Fredenhagen, Phys. Lett. B **483** (2000) 217 [hep-ph/0004145].

[39] W. Buchmuller and M. Plumacher, Phys. Lett. B **389** (1996) 73 [hep-ph/9608308].

[40] L. Covi, E. Roulet and F. Vissani, Phys. Lett. B **384** (1996) 169 [hep-ph/9605319].

[41] M. Flanz, E. A. Paschos and U. Sarkar, Phys. Lett. B **345** (1995) 248 [Erratum-ibid. B **382** (1996) 447] [hep-ph/9411366].

[42] W. Buchmuller and M. Plumacher, Phys. Lett. B **431** (1998) 354 [hep-ph/9710460].

[43] W. Buchmuller and T. Yanagida, Phys. Lett. B **445** (1999) 399 [hep-ph/9810308].

[44] S. Davidson and A. Ibarra, Phys. Lett. B **535** (2002) 25 [hep-ph/0202239].

[45] K. Hamaguchi, H. Murayama and T. Yanagida, Phys. Rev. D **65** (2002) 043512 [hep-ph/0109030].

[46] W. Buchmuller, P. Di Bari and M. Plumacher, Annals Phys. **315** (2005) 305 [hep-ph/0401240].

[47] W. Buchmuller, P. Di Bari and M. Plumacher, Nucl. Phys. B **643** (2002) 367 [Erratum-ibid. B **793** (2008) 362] [hep-ph/0205349].

[48] For recent reviews see, for example,
S. Davidson, E. Nardi and Y. Nir, "Leptogenesis," Phys. Rept. **466** (2008) 105 [0802.2962 [hep-ph]]; S. Blanchet and P. Di Bari, "The minimal scenario of leptogenesis," 1211.0512 [hep-ph]; T. Hambye, "Leptogenesis: beyond the minimal type I seesaw scenario," 1212.2888 [hep-ph]; G. C. Branco and M. N. Rebelo, "Leptonic CP violation and neutrino mass models," New J. Phys. **7** (2005) 86 [hep-ph/0411196].

[49] W. Buchmuller, V. Domcke and K. Schmitz, Nucl. Phys. B **862** (2012) 587 [1202.6679 [hep-ph]].

[50] M. Y. .Khlopov and A. D. Linde, Phys. Lett. B **138** (1984) 265.

[51] J. R. Ellis, J. E. Kim and D. V. Nanopoulos, Phys. Lett. B **145** (1984) 181.

[52] M. Bolz, A. Brandenburg and W. Buchmuller, Nucl. Phys. B **606** (2001) 518 [Erratum-ibid. B **790** (2008) 336] [hep-ph/0012052].

[53] J. Pradler and F. D. Steffen, Phys. Lett. B **648** (2007) 224.

[54] G. Lazarides and Q. Shafi, Phys. Lett. B **258** (1991) 305.

[55] H. Murayama, H. Suzuki, T. Yanagida and J. 'i. Yokoyama, Phys. Rev. Lett. **70** (1993) 1912.

[56] T. Asaka, K. Hamaguchi, M. Kawasaki and T. Yanagida, Phys. Lett. B **464** (1999) 12 [hep-ph/9906366]; Phys. Rev. D **61** (2000) 083512 [hep-ph/9907559].

[57] S. Antusch, J. P. Baumann, V. F. Domcke and P. M. Kostka, JCAP **1010** (2010) 006 [1007.0708 [hep-ph]].

[58] W. Buchmuller, K. Schmitz and G. Vertongen, Phys. Lett. B **693** (2010) 421 [1008.2355 [hep-ph]]; Nucl. Phys. B **851** (2011) 481 [1104.2750 [hep-ph]].

[59] E. J. Copeland, A. R. Liddle, D. H. Lyth, E. D. Stewart and D. Wands, Phys. Rev. D **49** (1994) 6410 [astro-ph/9401011].

[60] G. R. Dvali, Q. Shafi and R. K. Schaefer, Phys. Rev. Lett. **73** (1994) 1886 [hep-ph/9406319].

[61] M. Fujii, K. Hamaguchi and T. Yanagida, Phys. Rev. D **65** (2002) 115012 [hep-ph/0202210].

[62] G. N. Felder, J. Garcia-Bellido, P. B. Greene, L. Kofman, A. D. Linde and I. Tkachev, Phys. Rev. Lett. **87**, 011601 (2001), [hep-ph/0012142].

[63] M. Hindmarsh, Prog. Theor. Phys. Suppl. **190**, 197 (2011), arXiv:1106.0391 [astro-ph.CO].

[64] E. J. Copeland, S. Pascoli and A. Rajantie, Phys. Rev. D **65**, 103517 (2002), [hep-ph/0202031].

[65] K. Nakayama, F. Takahashi and T. T. Yanagida, JCAP **1012**, 010 (2010), 1007.5152 [hep-ph].

[66] R. Battye and A. Moss, Phys. Rev. D **82**, 023521 (2010), 1005.0479 [astro-ph.CO].

[67] J. Urrestilla, N. Bevis, M. Hindmarsh and M. Kunz, JCAP **1112**, 021 (2011), 1108.2730 [astro-ph.CO].

[68] C. Dvorkin, M. Wyman and W. Hu, Phys. Rev. D **84**, 123519 (2011), 1109.4947 [astro-ph.CO].

[69] E. Komatsu *et al.* [WMAP Collaboration], Astrophys. J. Suppl. **192**, 18 (2011), 1001.4538 [astro-ph.CO].

[70] J. Garcia-Bellido and E. Ruiz Morales, Phys. Lett. B **536**, 193 (2002), [hep-ph/0109230].

[71] J. Berges, D. Gelfand and J. Pruschke, Phys. Rev. Lett. **107**, 061301 (2011), 1012.4632 [hep-ph].

[72] M. Ibe and T. T. Yanagida, Phys. Lett. B **709** (2012) 374 [1112.2462 [hep-ph]]; M. Ibe, S. Matsumoto and T. T. Yanagida, Phys. Rev. D **85** (2012) 095011 [1202.2253 [hep-ph]].

[73] K. S. Jeong, M. Shimosuka and M. Yamaguchi, JHEP **1209** (2012) 050 [1112.5293 [hep-ph]].

[74] T. Gherghetta, G. F. Giudice and J. D. Wells, Nucl. Phys. B **559** (1999) 27, [hep-ph/9904378].

[75] M. Ibe, R. Kitano, H. Murayama and T. Yanagida, Phys. Rev. D **70** (2004) 075012, [hep-ph/0403198].

[76] N. Arkani-Hamed, A. Delgado and G. F. Giudice, Nucl. Phys. B **741** (2006) 108, [hep-ph/0601041].

[77] J. Hisano, S. Matsumoto, M. Nagai, O. Saito and M. Senami, Phys. Lett. B **646** (2007) 34, [hep-ph/0610249].

[78] M. Cirelli, A. Strumia and M. Tamburini, Nucl. Phys. B **787** (2007) 152, 0706.4071 [hep-ph].

[79] M. Kawasaki, K. Kohri, T. Moroi and A. Yotsuyanagi, Phys. Rev. D **78** (2008) 065011, 0804.3745 [hep-ph].

[80] W. Buchmuller, V. Domcke and K. Schmitz, Phys. Lett. B **713** (2012) 63 [1203.0285 [hep-ph]].